MICROWAVE SPECTROSCOPY ON A DOUBLE QUANTUM DOT

W.G. VAN DER WIEL[a], T. FUJISAWA[a,b], S. TARUCHA[b,c], T.H. OOSTERKAMP[a], R. AGUADO[a], R.M. SCHOUTEN[a], AND L.P. KOUWENHOVEN[a]

[a] Department of Applied Physics and Delft Institute of Microelectronics and Submicron-technology (DIMES), Delft University of Technology, P.O. Box 5046, 2600 GA Delft, The Netherlands

[b] NTT Basic Research Laboratories, 3-1, Morinosato-Wakamiya, Atsugi, Kanagawa, 243-0198, Japan

[c] Department of Physics, University of Tokyo, 7-3-1 Hongo, Bunkyo-ku, Tokyo 113-0033, Japan

Semiconductor quantum dots are often referred to as artificial atoms since they contain well-defined discrete levels. When two of these quantum dots are coupled, bonding and anti-bonding states are formed, analogous to covalent diatomic molecules. We use microwaves to excite an electron from the bonding to the anti-bonding state and measure a photon-assisted-tunneling current through a quantum dot molecule. We can change the tunnel coupling in-situ and find a clear transition from an electrostatic (ionic) to a covalent coupling in the double-quantum-dot system.

1 Introduction

Semiconductor quantum dots, in which charge states and single particle energy states are well defined in a zero-diminsional confinement potential, have been extensively studied to explore their electron states in analogy with real atoms[1]. When two of these quantum dots are coupled, the electrostatic coupling and the coherent tunneling coupling are the dominant coupling mechanisms[2-5]. The electrostatic coupling ionizes one quantum dot (attracts or repels an electron) to gain the electrostatic coupling energy. This resembles ionic diatomic molecules. The electrostatic coupling in a double quantum dot has been well discussed, especially in electron pump devices. The coherent tunneling coupling delocalizes the electron wavefunction spreading it over the two dots, and splits energy levels into bonding and anti-bonding levels in analogy to covalent diatomic molecules. The coherent coupling has been clearly observed in quantum well structures and superconducting tunneling devices[6,7]. However, the electrostatic bonding energy is usually larger than the covalent bonding energy in most lateral double dot devices. In this article, we measure the dc transport under microwave irradiation to directly detect the covalent coupling energy. The covalent coupling energy can be changed by gate voltages and/or magnetic field.

2 Double Quantum Dot System

We use two quantum dots, L and R, coupled in series fabricated in an AlGaAs/GaAs modulation doped heterostructure as schematically shown in Fig. 1(a) [8,9]. The central gate voltage, V_{GC}, and the magnetic field is used to modify the coupling strength between the dots. Negative gate voltages, V_{GL} on G_L and V_{GR} on G_R, are used to change the number of electons, N_L, in the dot L and N_R in the dot R, and to lift the discrete energy levels in the dots L and R. Typical energy spacing of the single particle states is 0.2 meV for dot R and 0.5 meV for dot L, which are larger than the energy regime investigated in the following measurements. Thus, we can consider only the lowest empty state of each dot for the tunneling current.

When the electrostatic tunneling coupling between the dots is significant, the transport is dominated by a sequential single-electron tunneling process; first an electron tunneling from the source to the dot L changes the charge state from the initial, ($N_L - 1$, $N_R - 1$), to the next, (N_L, $N_R - 1$), and forms an energy state, E_L; the second electron tunneling from dot L to dot R forms the charge state, ($N_L - 1$, N_R), and another energy state, E_R; then the electron in the dot R escapes to the drain to go back to the initial charge state. This is called the electron-like process, while the other tunneling process with one more electron in double dot is called hole-like process, in which the charge state changes from (N_L, N_R) through (N_L, $N_R - 1$) to ($N_L - 1$, N_R). Since these charge state are well defined by large charging energies and a significant electrostatic coupling between the dots, the two tunneling processes can be distinguished well [8]. If discrete energy levels are well defined in each dot, the tunneling is dominated by resonant tunneling between discrete levels [10].

When T is larger than Γ_R or other dephasing rates, an electron tunnels back and forth coherently between the two charge states, (N_L, $N_R - 1$) and ($N_L - 1$, N_R). The coherent oscillation over the two dots leads to two covalent states in analogy to covalent diatomic molecules. The bare uncoupled states, E_L and E_R, are split into a bonding state, E_B, and an anti-bonding state, E_A, as schematically illustrated in Fig. 1(b). The energy spacing of the coupled states, $\Delta E \equiv E_A - E_B$, is given by

$$\Delta E = \sqrt{\varepsilon^2 + (2hT)^2}; \qquad (1)$$

where $\varepsilon \equiv E_L - E_R$ is the energy spacing of the uncoupled states. It should be noted that the wavefunctions of the coupled states, Ψ_B for the bonding and Ψ_A for the anti-bonding state, are superpositions of the uncoupled states,

Figure 1: (a) Schematic diagram of the double quantum dot de¯ned in the 2DEG of a AlGaAs/GaAs hetero structure. The focused ion beam implantation and surounding depletion (cross hatched regions) de¯ne a narrow channel connecting to the source and the drain contacts. Negative voltages on the metal gates, G_L, G_L and G_L, induce tunable tunneling barriers and two quantum dots, L and R. The two quantum dots, L and R, respectively, contain »15 and »25 electrons; charging energies are »4 and »1meV; and the measured average spacing between single-particle states are »0.5 and »0.25 meV. (b) Energy diagram (vertical axis) along the spacial axis through the dots (horizontal axis). Thick vertical lines denote tunneling barriers. The dashed lines represents energies and schematic wavefunctions of the uncoupled states, $\tilde{A}_L$ and $\tilde{A}_R$, whose eneries are separated by ". The solid lines represent energies and schematic wavefunctions of the coupled states, bonding state, $\tilde{A}_B$, and anti-bonding state, $\tilde{A}_A$. The energy spacing, ¢E, is given by $¢E = \sqrt{"^2 + (2hT)^2}$. (c) Energy levels of the bonding state, E_B, and the anti-bonding state, E_A, versus ". The dahsed lines represents the energy levels of the uncoupled states. When a microwave ¯eld (frequency f) is irradiated, transition from the symmetric state to the anti-symmetric state takes place at the resonance, ¢E = hf, indicated by arrows.

Ψ_L and Ψ_R; i.e., $\Psi_B = \Psi_L \sin\theta + \Psi_R \cos\theta$, $\Psi_A = \Psi_L \cos\theta - \Psi_R \sin\theta$, where $\theta = \tan^{-1}((\Delta E - \varepsilon)/2hT)$ is the coupling angle of the two states.

3 Photon Assisted Tunneling Spectroscopy

Figure 1(c) shows the energies of the coupled states, E_B and E_A, with a significant tunneling coupling, T. When the double dot is irradiated by microwave, photon assisted tunneling (PAT) from the bonding to the anti-bonding state can be measured at the resonance, $\Delta E = hf$, where f is the microwave frequency. On the other hand, the gate voltages change the electrostatic potentials of the dots, which are responsible for the uncoupled states, E_L and E_R. Thus, the photon assisted tunneling resonances for various frequency and gate voltages give a complete energy spectrum of the double quantum dot[11,12].

Figure 2 shows a PAT current spectrum measured at a small bias voltage. The gate voltages, V_{GL} and V_{GR}, are swept in opposite directions to change ε, which is calibrated from the bias voltage or the PAT peak positions at higher frequencies. We chose the condition such that the Fermi energies, μ_S and μ_D, are located between the bonding and the anti-bonding state, to measure zero current without microwave irradiation. When the double dot is irradiated, the positive and the negative peaks appear as an excitation from the bonding to the anti-bonding state. We choose a minimum microwave power to make sure the coherent coupling is not disturbed[13]. In the regime where the PAT current is much smaller than the zero-photon current at finite bias voltage, the peak position is insensitive to the power, while current is proportional to the power. Since the wavefunctions have different weights on each of the dots at $\varepsilon \neq 0$, the electron tunnels either from the drain through coupling states to the source (positive current as shown in the right inset), or from the source through coupling states to the drain (negative current as shown in the left inset). At $\varepsilon = 0$, the coupled wavefunctions have equal weight on both dots, so that the net tunneling current is zero.

The peak positions do not show a linear dependence on the frequency, f, (dashed lines), but show a hyperbolic dependence (solid line fitted by eq. (1)). This clearly shows that the two quantum dots are coherently coupled with a covalent coupling energy of $2hT = 36\ \mu\text{eV}$. No PAT current is observed when the photon energy is decreased below the coupling energy, i.e. $hf < 2hT$.

The coupling energy can be decreased by applying a more negative voltage on the central gate or by applying a magnetic field. In Fig. 3 the peak position of the PAT spectrum is plotted as a function of frequency. Different symbols correspond to different gate voltages and different magnetic field. The solid lines are hyperbolic curves of eq. (1) fitted to the measured data. The covalent

Figure 2: (a) Measured photon assisted tunneling current through a coherently coupled double quantum dot. Gate voltages on G_L and G_R are swept simultaneously to give a energy difference, $\epsilon \equiv E_L - E_R$, between the two levels. The different traces are taken at different microwave frequencies and offsets are given such that the vertical axis gives the frequency. Typical peak current is 0.5 pA. The dashed lines shows a linear dependence, $\epsilon = hf$, expected to have no coherent coupling, while the solid curve is a hyperbolic dependence with a covalent energy of 36 μeV. The left and right insets show schematic energy diagrams to show different current directions. At positive ϵ, the bonding and anti-bonding states have weighted respectively on the left dot and the right dot, and vice versa at negative ϵ. (b) The microwave frequency, f, dependence of the resonance condition, ϵ, taken by half of the energy spacing between the positive and the negative peaks. Different symbols taken with different gate voltages and magnetic field (² : 7 T, ± : 3.3 T, 2 : 2.2 T, and other symbols : 0T). Solid lines are the hyperbolic dependence fits to the data.

energy is controlled from »0 to 60 ¹eV by gate voltages and/or magnetic ¯eld. The clear hyperbolic dependence on " shows that the localized state, $\tilde{A}_L$ and $\tilde{A}_R$, can be mixed with the coupling angle, µ. The microwave absorption process in our experiment is a transition from one coupling angle, µ to the other, µ ¡ ¼=2. If absorption and stimulated emission take place coherently, Rabi oscillations are expected in the PAT response [12]. This implies that the coupling angle can be controlled by a short time period of the microwave irradiation, as is done in Rydberg atoms [14].

We didn't mention the electrostatic coupling, which can be measured by conventional dc transport technique but not from the microwave spectroscopy. It is noted that the electrostatic coupling is also a®ected by gate voltages and magnetic ¯eld.

4 Summary

In summary we have discussed coherent tunneling coupling between two quantum dots. The microwave excitation measurement detects the covalent coupling energy, which is an energy spacing between the bonding and anti-bonding energies. We demonstrated a clear transition from ionic (T » 0) to covalent (T = 60 ¹ eV) coupling.

Acknowledgments

We thank S.M. Cronenwett, S.F. Godijn, P. Hadley, K. Ishibashi, C.J.P.M. Harmans, K.K. Likharev, J.E. Mooij, Yu. V. Nazarov, T.H. Stoof and N.C. van der Vaart for experimental help and useful discussions. This work was supported by the Dutch Organization for Research on Matter (FOM) and by the EU via the TMR network. L.P.K. was supported by the Dutch Royal Academy of Arts and Sciences (KNAW). S.T. was supported by a Grant-in-Aid for Scienti¯c Research on the Priority Area "Spin Controlled Semiconductor Nanostructures" (No. 09244103) from the Ministry of Education, Science, Sports, and Culture.

References

1. For a review, see L. P. Kouwenhoven et al., in Mesocopic Electron Transport, Proceedings of a NATO Advanced Study Institute, L.L. Sohn, L.P. Kouwenhoven, and G. Schön, Eds., (Kluwer, Dordrecht, 1997), ser. E, vol. 345, pp. 105-214; available on line at http://vortex.tn.tudelft.nl/~leok/papers/.
2. N.C. van der Vaart et al., Phys. Rev. Lett. 74, 4702 (1995).

3. F.R. Waugh et al., Phys. Rev. Lett. 75, 705 (1995).
4. C. Livermore et al., Science 274, 1332 (1996).
5. R. Blick et al., Phys. Rev. B 53, 7899 (1996).
6. L.P. Kouwenhoven et al., Phys. Rev. Lett. 66, 201 (1991).
7. Y. Nakamura, C.D. Chen, and J.S. Tsai, Phys. Rev. Lett. 79 ,2328 (1997).
8. T. Fujisawa and S. Tarucha, Superlattices and Microstructures 21, 247 (1997); Jpn. J. Appl. Phys. 36, 4000 (1997).
9. A large part of this manuscript is also being published in: T.H. Oosterkamp, et al. to be published in Nature and T. Fujisawa et al., Proceedings of the IEEE Twenty-Fifth International Symposium on Compound Semiconductors, Nara, Japan (1998, submitted).
10. L.P. Kouwenhoven et al., Science 275, 1896 (1997).
11. T.H. Stoof and Yu. V. Nazarov, Phys. Rev. B 53, 1050 (1996).
12. C.A. Sta®ord and N.S. Wingreen, Phys. Rev. Lett. 76, 1916 (1996).
13. The e®ective tunneling coupling can be reduced by zeroth order Bessel function [12].
14. M. Brune, Phys. Rev. Lett. 76, 1800 (1996).

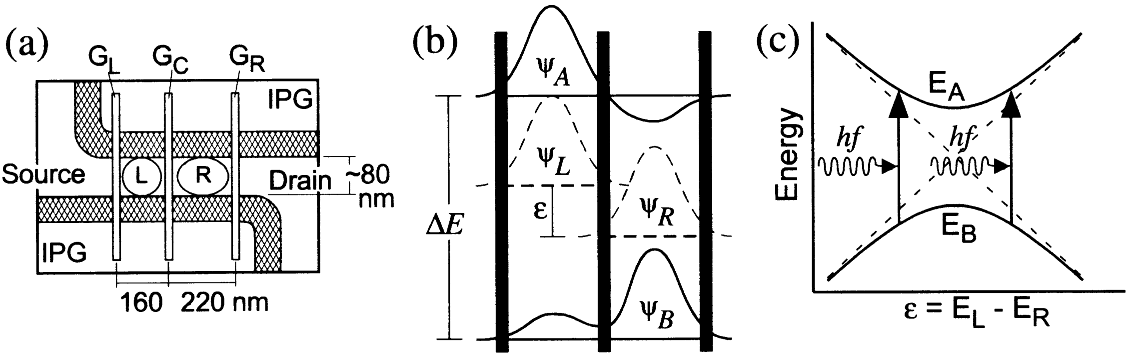
(a)
G_L
G_C
G_R
IPG
Source
L
R
Drain
~80 nm
IPG
160
220 nm
(b)
ψ_A
ψ_L
ψ_R
ψ_B
ε
ΔE
(c)
E_A
E_B
hf
hf
Energy
$\varepsilon = E_L - E_R$

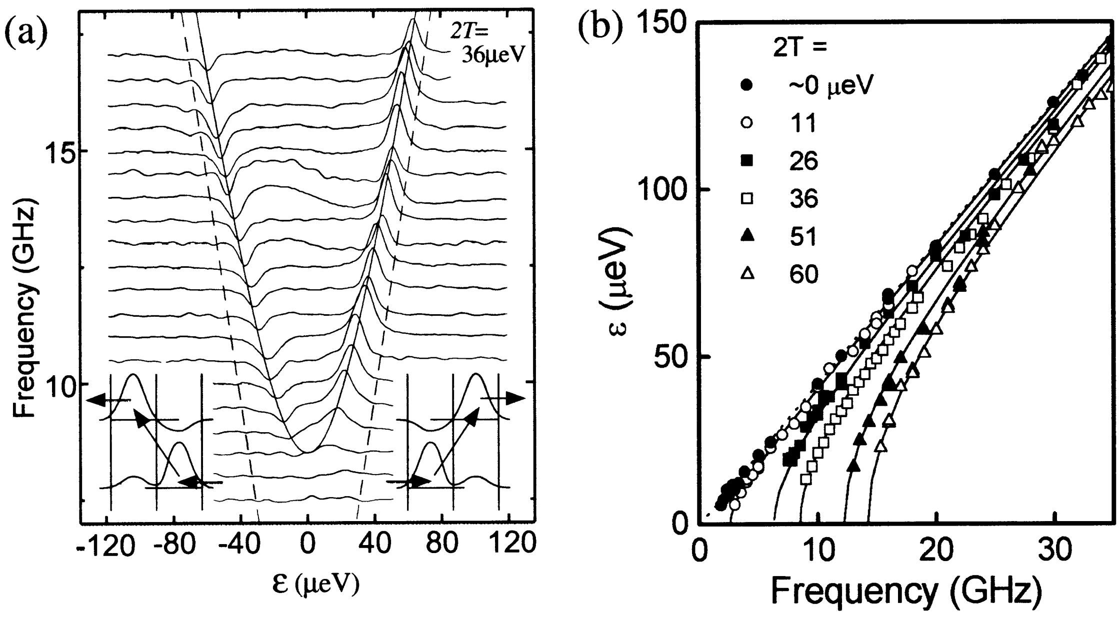
(a)
2T= 36μeV
Frequency (GHz)
15
10
-120
-80
-40
0
40
80
120
ε (μeV)
(b)
2T =
~0 μeV
11
26
36
51
60
ε (μeV)
150
100
50
0
0
10
20
30
Frequency (GHz)